THE ASTROPHYSICAL JOURNAL, 401:L39–L42, 1992 December 10

VLBI OBSERVATIONS OF THE 6.7 GHz METHANOL MASERS TOWARD W3(OH)

K. M. MENTEN, M. J. REID, P. PRATAP, AND J. M. MORAN
Harvard-Smithsonian Center for Astrophysics, 60 Garden Street, Cambridge, MA 02138
AND
T. L. WILSON
Max-Planck-Institut für Radioastronomie, Auf dem Hügel 69, 5300 Bonn 1, Germany
Received 1992 August 14; accepted 1992 September 24

ABSTRACT

We have conducted very long baseline interferometric (VLBI) observations of the 6.668 GHz maser transition of interstellar methanol toward the ultracompact H II region W3(OH). We have determined absolute maser positions with an accuracy of 0.″05 and produced maps that show that the methanol masers have a distribution similar to the hydroxyl masers in this source. The intrinsic sizes of individual maser spots are $\approx$0.″0014 (FWHM), or $\approx$3 AU, and are not significantly affected by interstellar scattering. By comparing maps of the 6.7 and 12.2 GHz methanol maser transitions, we find that the maps can be aligned so that the positions of the strongest 6.7 GHz emission features agree to within a maser spot size ($\approx$0.″001) with the positions of strong 12.2 GHz features at the same velocities. This result will provide strong constraints on any excitation mechanism for class II methanol masers.

Subject headings: H II regions — ISM: molecules — masers — radio lines: ISM — stars: formation — techniques: interferometric

1. INTRODUCTION

Class II methanol (CH_3OH) masers (Batrla et al. 1987; Menten 1991a) are located in the dense, warm, molecular envelopes of ultracompact H II regions, the same environment that gives rise to hydroxyl (OH) masers. The strongest Class II maser transitions are the $2_0 \rightarrow 3_{-1}E$ line near 12.2 GHz (Batrla et al. 1987) and, most prominently, the recently detected $5_1 \rightarrow 6_0\,A^+$ line near 6.7 GHz (Menten 1991b). High-resolution observations of these masers can provide important information on the physical and chemical conditions in their emitting regions, which are determined by the interaction of the newly formed high-mass stars with their environment. Recently, we conducted a VLBI experiment to obtain milliarcsecond resolution observations of the 6.7 GHz methanol masers toward a number of star-forming regions. In this *Letter* we present the results of our observations toward the archetypical ultracompact H II region/maser source W3(OH).

In the past, W3(OH) has been studied with VLBI methods in various OH lines, most extensively in the 1665 MHz $^2\Pi_{3/2}$, $J = 3/2$, $F = 1 \rightarrow 1$ transition (e.g., Reid et al. 1980, García-Barreto et al. 1988; Bloemhof, Reid, & Moran 1992), as well as in the 12.2 GHz CH_3OH transition (Menten et al. 1988a). Some objectives of our VLBI study were to obtain subarcsecond absolute position information for the 6.7 GHz masers, to map the distribution of the maser emission and compare it with existing maps of the OH and 12.2 GHz CH_3OH masers, and to derive apparent sizes for the maser spots. Such multitransition studies of masers have great scientific potential. In particular, a comparison of the 6.7 and 12.2 GHz emitting regions can, in principle, yield important information on the maser excitation mechanism, while a comparison of maser spot sizes determined at different wavelengths can be used to decide whether the observed sizes are intrinsic or the result of broadening by interstellar scattering.

2. OBSERVATIONS AND DATA ANALYSIS

The VLBI experiment was conducted between 1992 April 15 and 20 with the NRAO[1] 43 m antenna in Green Bank, WV, the Haystack 37 m antenna in Westford, MA, and the MPIfR 100 m telescope in Effelsberg, Germany. The rest frequency of the $5_1 \rightarrow 6_0\,A^+$ transition is 6668.518 $\pm$ 0.005 MHz (Menten 1991b) and the minimum fringe spacings were 0.″011 for the short (NRAO-Haystack) baseline and 0.″0015 for the longest (NRAO-Effelsberg) baseline. The NRAO antenna recorded linear polarization (position angle of *E*-vector 67.°5 east of north) while the Haystack and Effelsberg antennas recorded left circular polarization. The observing cycle of a 20 minute observation of a maser source followed by a 10 minute observation of an extragalactic continuum source was repeated throughout the observations. A 500 kHz band centered at an LSR velocity of -44 km s^{-1} was recorded using the Mk II VLBI system. The data were correlated on the NRAO Mk II VLBI processor at Socorro, NM using 192 complex cross-correlation lags and 96 real autocorrelation lags, giving 96 point spectra with uniformly weighted spectral channels separated by 0.234 km s^{-1}. The relative offsets and drift rates of the station clocks were determined from the continuum source observations and the maser positions were measured from the fringe-rate residuals. Values for the polar motion and UT1-UTC values were taken from the USNO circular. For W3(OH) the absolute position of the reference feature, at a velocity of -45.4 km s^{-1}, was determined to be $(\alpha, \delta)_{1950} = 2^h23^m16^s.456 \pm 0^s.008, +61°38'57''.76 \pm 0''.05$. The spectral line VLBI data were calibrated in amplitude and phase using the techniques described by Reid et al. (1980). The absolute flux

[1] The National Radio Astronomy Observatory is operated by Associated Universities, Inc., under a cooperative agreement with the National Science Foundation.

density scale was determined using the data of Menten (1991b) and radiometry at the Green Bank telescope. We used the multiple point fringe-rate mapping technique to determine positions of the maser features relative to the above mentioned reference feature. In addition, we produced aperture synthesis maps from the phase referenced data using only visibilities from the NRAO-Haystack baseline. For a high declination source, such as W3(OH), a single long track with one baseline produces a ringlike UV coverage.

For all velocity channels containing emission we produced maps of size 2".56 × 2".56 centered 0".76 south of the position of the reference feature quoted above, thus covering a region that is known to contain all of the emission detected in other CH_3OH and OH transitions. These maps were made and CLEANed using the NRAO AIPS software. Because of the limited UV coverage of the observations, our synthesis maps have relatively low dynamic range ($\approx$15:1) even after CLEANing and velocity channels containing very intense emission are heavily confused by incompletely removed spatial side lobes of these strong features. In addition, spectral "ringing" resulting from strong maser spikes that are unresolved with our relatively coarse spectral resolution of 0.234 km s^{-1} can produce spurious features in neighboring channels. We Hanning-weighted the data before mapping to reduce these spectral side lobes. To assess the reality of a given maser feature in an unbiased way, we only considered a feature to be real if it satisfied the following two criteria: first, its flux density had to be greater than 6 times the rms flux density in at least two adjacent channels, and, second, its flux density had to be $\geq$7% of the peak flux density in each of these channels. The second criterium, which corresponds to a dynamic range limit of 15:1, was determined by visual inspection of several maps. Using these criteria, certainly some "real" features were rejected since the peak flux density in a given channel varies dramatically from channel to channel. Therefore, a feature that is well above the dynamic range cutoff level in one channel may be rejected in its neighboring channels, thus not satisfying the first requirement.

To compare the emission distribution in the 6.7 and 12.2 GHz methanol lines, we produced synthesis maps from the 12.2 GHz data of Menten et al. (1988a), using similar mapping and analysis procedures as in the case of the 6.7 GHz data. Note that the 12.2 GHz positions presented by Menten et al. (1988a) were determined using less sensitive fringe-rate mapping methods. In the 6.7 and 12.2 GHz maps maser positions were determined by two-dimensional Gaussian fitting. Errors in the relative positions of maser spots are $\lesssim$0".001.

3. RESULTS AND DISCUSSION

In Figure 1 we compare cross-power spectra from our short baseline and one long baseline with a total-power spectrum of the maser emission toward W3(OH). The shape of the total power spectrum is identical to that of the spectrum taken by Menten (1991b) in 1991 June if the latter is smoothed to the same effective velocity resolution. Like the 12.2 GHz masers, the 6.7 GHz line seems to exhibit little or no temporal variability. Circular and linear polarization spectra are identical to within our uncertainties, suggesting that any polarization of the maser radiation is small. Somewhat surprisingly, the visibilities on even the short baseline are rather low, which might be due to destructive interference of several strong features blended together spectrally. However, the total flux density in our synthesis maps (Fig. 1, *upper panel*) accounts for less than

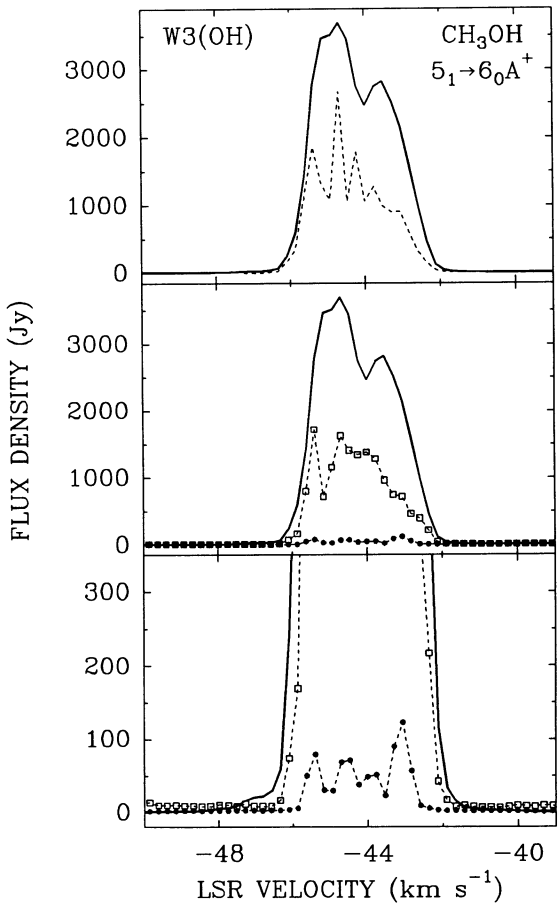

FIG. 1.—Spectra of the 6.7 GHz $5_1 \rightarrow 6_0 A^+$ line of methanol toward W3(OH). In all panels the thick solid line represents a total power spectrum. In the upper panel the dashed line shows the flux density summed over all maser features identified in our synthesis maps as described in the text. In the middle panel the open squares and the filled circles connected by dashed line represent cross-power spectra from the NRAO-Haystack and NRAO-Effelsberg baselines, respectively. Both cross-power spectra result from observations made on 1992 April 17, 11:07 U.T. The lower panel is a blow-up of the middle panel. The spectra are Hanning-smoothed to an effective velocity resolution of 0.47 km s^{-1}.

half the flux density in the total power spectrum. The missing flux density could arise from spatial structures significantly larger than the maximum fringe spacing of our experiment. By fitting a circularly symmetric Gaussian model to the observed variation of the fringe visibilities with baseline length, we determine a characteristic size of 0".0014 (FWHM) for our reference feature, corresponding to 3 AU, if we assume a distance of 2.2 kpc (Humphreys 1978). The inferred brightness temperature is 3×10^{12} K. The measured source size is approximately the same as for the 12.2 GHz methanol masers (see Menten et al. 1988a) and the 1665 MHz OH masers, for which the more compact spots have sizes $\lesssim$ 0".003 (Reid et al. 1980). Since a variation of the source size proportional to the square of the wavelength would be expected if scattering were important (see, e.g., Gwinn et al. 1988), we conclude that the observed spot sizes for both methanol transitions, and probably for the OH masers, are intrinsic sizes and not the result of interstellar scattering.

The results of our synthesis mapping are presented in Figure 2, where we show the distribution of 6.6 GHz maser spots

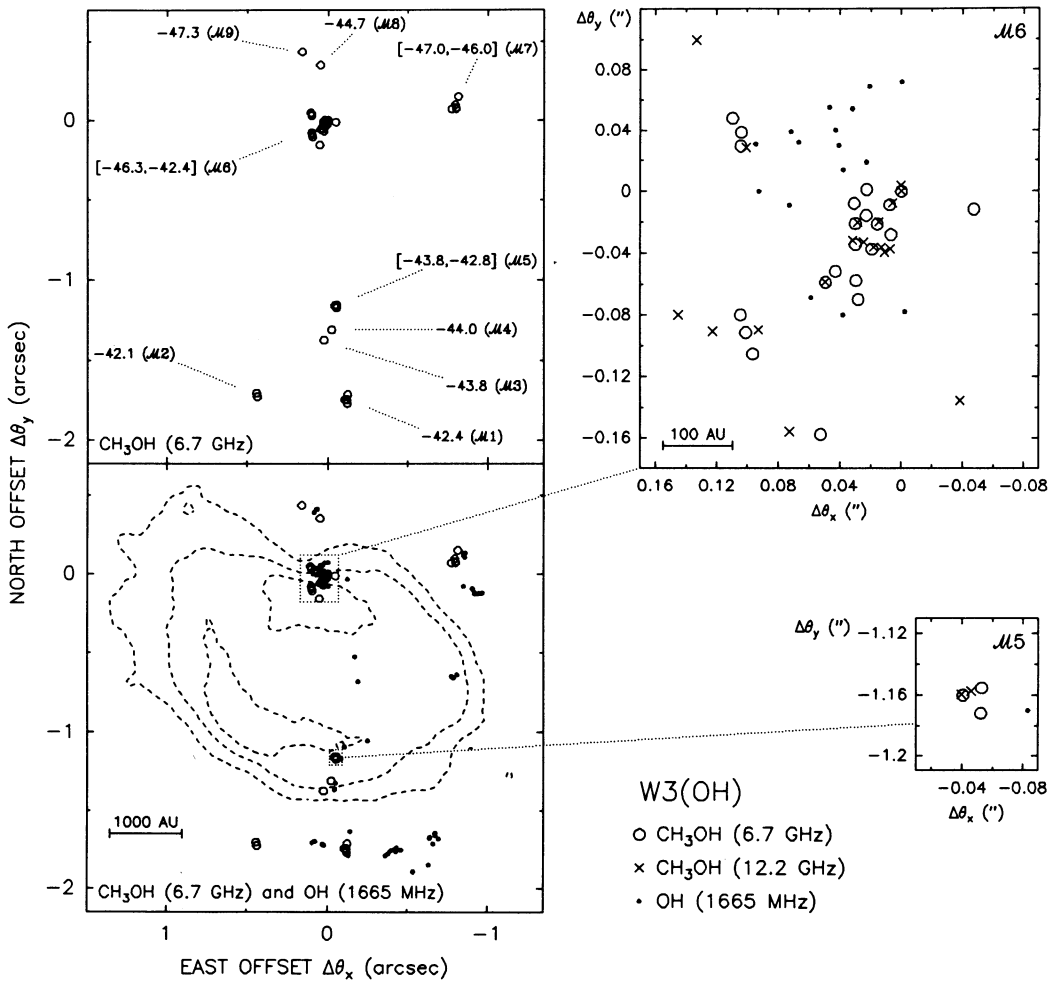

FIG. 2.—Angular distribution of maser emission toward W3(OH). In all panels the open circles mark the positions of the 6.7 GHz CH_3OH masers. In the upper left-hand panel their velocities are indicated and maser clusters are numbered ($M1$ to $M9$) for reference in the text. In cases where a single velocity is given for a cluster containing several maser spots, the velocities of the individual features were all within 0.5 km s^{-1} and the centroid velocity is shown. Three clusters have larger velocity spreads, which are listed in the square brackets. In the lower left-hand panel the positions of 6.7 GHz CH_3OH and 1665 MHz OH masers (*small dots*) are plotted on top of dashed contour lines that represent the 0.5, 7.1, and 16.6 mJy $beam^{-1}$ levels of a VLA 2 cm continuum map kindly provided by C. Masson. For the OH masers, relative positions were measured by García-Barreto et al. (1988), while absolute positioning was obtained by using the reference feature position of Reid et al. (1980), which has an uncertainty of 0".1 in each coordinate. All position offsets are relative to position of the 6.7 GHz CH_3OH reference feature at $v_{LSR} = -45.4$ km s^{-1}. The two panels on the right-hand side represent blow-ups of the regions (*dotted lines*) containing maser emission from *both* the 6.7 and 12.2 GHz CH_3OH lines. The 6.7 and 12.2 GHz CH_3OH maser positions are denoted as open circles and crosses, respectively, 1665 MHz OH masers as small dots. All relative position errors of methanol features are $\lesssim 1$ milliarcsecond, much smaller than the symbol sizes. As discussed in the text, the 12.2 GHz and 6.7 GHz reference features are assumed to have identical positions.

together with the positions of the 1665 MHz OH masers, the 12.2 GHz methanol masers, and the 2 cm wavelength continuum emission from the ultracompact H II region. Using the criteria discussed above, we identify 40 emission features distributed over an 1".3 × 2".2 area. Most of the features are clustered in a few regions identified as $M1$ to $M9$ in Figure 2. All of these clusters are smaller than 0".1 (200 AU) and have velocity spreads of less than 1 km s^{-1}, except for $M6$, which is by far the richest cluster, containing, in a 350 × 500 AU area, 22 features with velocities between −46.3 and −42.4 km s^{-1}.

The general distribution of the 6.7 GHz CH_3OH masers resembles closely that of the OH masers in W3(OH). In the lower part of Figure 2 we show an overlay of the methanol and 1665 MHz OH maser positions taken from García-Barreto et al. (1988). OH masers are found in or near all of the 6.7 GHz maser clumps, except for the easternmost clump $M2$. If one corrects the OH velocities for the shifts caused by the Zeeman effect (see Fig. 7 of Bloemhof et al. 1992), one finds that in all cases the velocities of neighboring OH and CH_3OH masers are the same within a few tenths of a km s^{-1}. We thus corroborate the result of Menten et al. (1988a, b) that Class II CH_3OH masers and OH masers arise from the same gas cloud.[2] This result is quite remarkable from a chemical point of view. While high OH abundances in the envelopes of ultracompact H II regions might be produced either in shocks (Elitzur & de Jong 1978) or photodissociation regions (Hartquist & Sternberg 1991), no model has yet been able to produce the high CH_3OH abundances found in these regions. Studying possible CH_3OH production processes in the photodissociation regime modeled

[2] Apparent differences in the OH and CH_3OH distribution on size scales $\lesssim 200$ AU, for example in region $M6$ (Fig. 2, *upper right panel*), seem to suggest a possible anticorrelation of OH and CH_3OH masers on small scales. However, since the absolute position of the OH masers has an uncertainty of 0".1 (≈ 200 AU) (Reid et al. 1980), a comparison of both species on these size scales has to await more accurate OH position determinations.

TABLE 1

6.7 GHz MASER COMPONENTS WITH 12 GHz COUNTERPARTS

6.7 GHz Line (measured on 1992 April 17).....				12.2 GHz Line (measured on 1988 April 9)....				
v_{LSR} (km s^{-1})	S_{peak} (Jy)	$\Delta\theta_x$ (mas)	$\Delta\theta_y$ (mas)	v_{LSR} (km s^{-1})	S_{peak} (Jy)	$\Delta\theta_x$ (mas)	$\Delta\theta_y$ (mas)	$\delta(\Delta\theta)$ (mas)
−43.1	756	49.54(0.07)	−58.65(0.05)	−43.0	10	49.78(0.14)	−58.46(0.14)	0.30(0.22)
−43.1	106	−34.81(0.32)	−1160.22(0.40)	−43.0	36	−34.38(0.03)	−1159.93(0.02)	0.50(0.51)
−44.0	991	19.37(0.07)	−37.48(0.05)	−43.8	102	18.17(0.02)	−36.33(0.01)	1.66(0.09)
−44.5	694	15.74(0.27)	−21.29(0.27)	−44.5	63	14.82(0.10)	−19.92(0.09)	1.65(0.41)
−44.9	374	7.59(0.72)	−8.86(0.55)	−44.7	187	5.89(0.03)	−7.53(0.03)	2.16(0.91)
−44.9	377	30.03(0.07)	−20.83(0.07)	−44.7	137	28.37(0.01)	−20.16(0.01)	1.80(0.10)
−45.4	1858	0.00	0.00	−45.2	221	0.00	0.00	...

NOTES.—$\Delta\theta_x$ and $\Delta\theta_y$ denote east and north offsets (equinox B1950, epoch 1950.0) in milliarcseconds (mas) from the reference feature listed in the bottom line. Errors in $\Delta\theta_x$ and $\Delta\theta_y$ are given in parentheses and are formal 1 σ deviations determined by Gaussian fits. Separations between corresponding 6.7 and 12.2 GHz features, $\delta(\Delta\theta)$, are given in the rightmost column. If these separations reflect internal motions over the 4 year period between the measurements, relative proper motion velocities between 0.8 and 5.6 km s^{-1} are inferred, comparable to values found for OH masers.

by Hartquist & Sternberg (1991) might be helpful in this respect.

When comparing the spatial distributions of the 6.7 and 12.2 GHz methanol masers we find, in agreement with Menten et al. (1988a), that 12.2 GHz maser emission arises from only two regions, which coincide with the areas of most prominent 6.7 GHz emission, namely the rich northern cluster $\mathcal{M}6$ and the region $\mathcal{M}5$ (1".1 south of $\mathcal{M}6$). The channels chosen for phase-referencing the 6.7 GHz and the 12.2 GHz data are at identical velocities and both contain a very strong maser feature. The absolute positions of the 6.7 and 12.2 GHz reference features agree within their joint uncertainties. If we assume that the 6.7 and 12.2 GHz reference features arise from *exactly* the same position, we find that another six of the strongest 12.2 GHz maser spots are also aligned (within 1–2 milliarcseconds) with strong 6.7 GHz features *at the same velocities*, within the uncertainties of the rest frequencies (see Table 1). More precisely, for the intensity range where our maps are considered complete given our dynamic range and sensitivity cutoff criteria, *every* 6.7 GHz feature has a 12.2 GHz counterpart at the same position and velocity and vice versa. In all cases the 6.7 GHz emission is stronger, and the 6.7 to 12.2 GHz flux density ratios for masers clearly detected in both lines range between 2 and about 80. Furthermore, we note that, most strikingly, the small offsets between 6.7 and 12.2 GHz features listed in Table 1 have the magnitude and orientation one would expect from proper motions, assuming the methanol masers have internal motions comparable to those measured for the OH masers by Bloemhof et al. (1992).

Several of the 6.7 GHz emission regions also show emission in the $9_2 \rightarrow 10_1 A^+$ transition of methanol near 23.1 GHz, which has been mapped at 0".08 resolution with the VLA (Menten et al. 1988b). The regions $\mathcal{M}4$ and $\mathcal{M}5$ both show 6.7 and 23.1 GHz emission at identical velocities. Some 23.1 GHz emission is also observed toward $\mathcal{M}6$, but with a smaller extent and much narrower velocity range than the 6.7 GHz emission. Several 23.1 GHz features located between $\mathcal{M}5$ and $\mathcal{M}6$ do not have 6.7 GHz counterparts. By far the strongest 23.1 GHz emission is observed toward $\mathcal{M}5$, in contrast to the 6.7 and 12.2 GHz lines, which both show their strongest features toward $\mathcal{M}6$.

While the dynamic range limitations of our 6.7 and 12.2 GHz maps could be responsible for some of the observed differences between the distributions of the 6.7, 12.2, and 23.1 GHz emission, it is nevertheless clear that the intensity ratios among these individual transitions show pronounced variations with position, reflecting different excitation conditions. Future higher dynamic range VLBI maps in both the 6.7 and 12.2 GHz line as well as in the higher frequency Class II transitions should produce valuable input for modeling efforts, which are currently hampered by the lack of reliable collisional rate coefficients. In particular, the fact that we are able to observe 6.7 and 12.2 GHz emission arising from the same maser cloudlets should put stringent constraints on any methanol maser excitation model. The close relationship between 6.7 and 12.2 GHz masers observed toward W3(OH) almost certainly also exists in other regions. This is suggested by the similarity of 6.7 and 12.2 GHz single-dish spectra (Menten 1991b) and radio-linked interferometric observations of Norris (1992).

We thank I. Shapiro for his enthusiastic support of this project. J. Carter, C. Papa, and E. Tong built the 6.7 GHz receiver and feed system for the Haystack telescope and A. Schmidt and K. Müller the Effelsberg receiver on short notice. We also thank J. Ball, J. Salah (Haystack), R. Schulze (MPIfR), C. Brockway, and G. Grove (NRAO) for support at the participating telescopes, C. Masson for providing the 2 cm continuum map of W3(OH), and T. Hartquist and the referee for helpful comments.

REFERENCES

Batrla, W., Matthews, H. E., Menten, K. M., & Walmsley, C. M. 1987, Nature, 326, 49
Bloemhof, E. E., Reid, M. J., & Moran, J. M. 1992, ApJ, 398, 500
Elitzur, M., & de Jong, T. 1978, A&A, 67, 323
Garcia-Barreto, J. A., Burke, B. F., Reid, M. J., Moran, J. M., Haschick, A. D., & Schilizzi, R. T. 1988, ApJ, 326, 954
Gwinn, C. R., Moran, J. M., Reid, M. J., & Schneps, M. H. 1988, ApJ, 330, 817
Hartquist, T. W., & Sternberg, A. 1991, MNRAS, 248, 48
Humphreys, R. M. 1978, ApJS, 38, 309
Menten, K. M. 1991a, in Skylines, Proceedings of the Third Haystack Observatory Meeting, ed. A. D. Haschick & P. T. P. Ho (San Francisco: ASP), 119
———. 1991b, ApJ, 380, L75
Menten, K. M., Johnston, K. J., Wadiak, E. J., Walmsley, C. M., & Wilson, T. L. 1988b, ApJ, 331 L41
Menten, K. M., Reid, M. J., Moran, J. M., Wilson, T. L., Johnston, K. J., & Batrla, W. 1988a, ApJ, 333, L83
Norris, R. P. 1992, in Astrophysical Masers, ed. A. Clegg & G. Nedoluha (Berlin: Springer), in press
Reid, M. J., Haschick, A., Burke, B. F., Moran, J. M., Johnston, K. J., & Swenson, G. W., Jr. 1980, ApJ, 239, 89